A COARSE-GRAINED TRANSPORT MODEL FOR NANO-FLUIDIC SYSTEMS

BY

NABIL RAMLAWI

THESIS

Submitted in partial fulfillment of the requirements
for the degree of Master of Science in Mechanical Engineering
in the Graduate College of the
University of Illinois at Urbana-Champaign, 2018

Urbana, Illinois

Adviser:

Professor Narayana Aluru

ABSTRACT

Molecular Dynamics (MD) is an important tool to simulate flows at the nanoscale. The limitation of MD in simulating important biological and chemical systems having a large length and time scale, increased the interest in efficient coarse-grained (CG) models. Although many existing CG models for various fluids are able to capture structure and dynamics of the bulk fluid accurately, these models are not suited to describe transport phenomena involving explicit walls in nano-channels. Previous coarse-grained models for confined fluids are only optimized to match the structure of the confined fluid. Here we introduce a complete CG transport model for a single component fluid in nano-channels having explicit walls. The model, which was applied to the water-graphene system, was able to demonstrate a very good match, with the structure (error$<$ 7%) and dynamical (error$<$1%) equilibrium properties of MD simulations. Moreover, the CG model was able to reproduce the MD results for water transport in a Poiseuille flow configuration with an error $<$ 5%. The accuracy of the model was transferable through different configurations and forcing conditions up to a critical force, where the MD slip velocity starts to deviate from the equilibrium prediction. Finally, the CG model was able to achieve $\approx$ 20x speedup compared to MD simulations, making it more suitable for flows close to experimental conditions, where MD produces a poor signal to noise ratio.

To my parents, for their love and support.

ACKNOWLEDGMENTS

The utmost gratitude and love goes to my parents, to whom I am indebted with everything I have. They nurtured and raised me to be the man I am today. They unconditionally gave everything to ensure my well-being and success. Their and my brother and sisters' love was able my heart even thousands of miles away. In short, this is their accomplishment, more than it is mine.

Secondly, I would like to thank my advisor Professor Narayana Aluru for his guidance and support. Prof. Aluru's thrive for excellence and integrity pushed me to work up to the best academic standards. His ideas and critical thinking contributed immensely to the work presented in this thesis.

Moreover, I would also like to thank my group mates, who always provided good company and positive criticism. Specifically, I would like to thank: Dr. Bhadauria for mentoring me and providing me with numerous useful scripts, Dr. Sikandar for his wise suggestions and meticulous skill in software installation, and Subhadeep, Houssein, Alireza and Mosi for being good friends in addition to being group mates.

Furthermore, the presence of extraordinary friends around kept me focused and happy. Special thanks go to the generous Ali, the irreproachable Hussein, the joyful Lina, the smart Hassan, my kindhearted dear cousin Ali, and all the great and beloved friends I met in Urbana-Champaign. I am also very grateful to my Oud teacher Fadi Alnaji for giving me the opportunity to learn to play and perform with my favorite instrument.

Finally, the ultimate praise is to God, whom He alone created me, this world, and destined all the factors to this achievement I mentioned above.

TABLE OF CONTENTS

LIST OF TABLES

LIST OF FIGURES

CHAPTER 1

INTRODUCTION

Molecular dynamics (MD) simulations, is a very powerful tool to study systems at the atomic level. From simulating just hundreds of atoms in the 70s[1] to simulating virus cells with about 1 million atoms recently[2], MD simulations have led to many groundbreaking discoveries (e.g., protein folding[3], DNA replication[4], and ultra-fast transport of water through nanopores[5]). In spite of the advancement in computational power, larger length and time scales are still inaccessible for MD. For example, the time scale of relevance exceeds microseconds for some systems such as viruses, cells and large protein chains[6]. Therefore, many attempts have been made to develop coarse-grained (CG) models that reduce the computational footprint of nano-scale simulations[7][8][9]. During coarse-graining, a set of atoms in the atomistic system are mapped into one particle at the center of mass of the atoms. Figure 1.1 shows a very simple example of how a water molecule can be coarse-grained. After mapping the atomistic system, a new effective potential between the CG molecules is optimized to match certain properties of interest, which is the main task of any coarse-graining procedure.

Structure-preserving coarse-graining techniques have been extensively developed for nano-fluidic systems. To replicate structure, a common practice is to choose the radial distribution function of the center of mass of the all-atom molecule derived from the all-atom MD simulations (AAMD), as a target for the CG system to imitate. The interaction potential can take a specific analytical form, based on physical motivation, or a numerical general form such as cubic splines, depending on the coarse-graining method used. Successful structural CG methods include Iterative

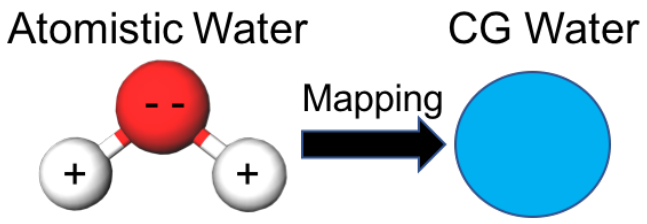

Figure 1.1: Illustration of how an atomistic water molecule representation that includes particle charges is mapped into a coarse-grained neutral molecule.

Boltzmann Inversion(IBI), Force Matching, and Relative Entropy[8][9][10]. CGMD simulations can be done using the same commercial packages used for the MD simulations. The only difference will be that the tabulated potentials produced by the CG procedure will be used as an inter-atomic potential between the CG particles, combined with a thermostat such as the Nose-Hoover(NH) thermostat. Moreover, when using the NH thermostat, CG methods developed to match the structure of the explicit system show tendency to have fast dynamics. Hence, the transport properties of these systems do not match the transport properties of the explicit atomistic system.

Many attempts have been made to slow the dynamics of the CG system by sampling the configuration space differently[11]. Changing the thermostat properties will preserve structure and provide the ability to tune the dynamical properties of the system. A commonly used thermostat is the dissipative particle dynamics(DPD) thermostat[12]. The DPD thermostat adds two extra types of interatomic forces: a dissipative force and a random force. The dissipative force will add a viscous effect between the particles while the random force puts back the energy dissipated by the dissipative force to satisfy fluctuation dissipation theorem. The magnitude of the dissipative force will set the viscosity and diffusion coefficient of the system. These methods were exclusively applied to bulk systems in previous works. Nevertheless, in nano-fluidic systems, the fluid is confined in small channels, giving rise to properties specific to the wall-fluid combination. For example, it is well-known that the layering of water over a hydrophobic Graphene sheet is different from the layering

over hydrophilic silicon. Moreover, the slip length observed for these two systems are different as well. A rigorous coarse-grained model should account for those properties and match them with the all-atom reference system.

Apart from systematic coarse-graining, dissipative particle dynamics is one of the mesoscopic methods used to simulate transport. DPD is a particle based method used to model fluids at the mesoscale. It was first developed by Hogelburge and Koleman in 1991 as an efficient particle based method, that is able to simulate the correct hydrodynamic behavior over a large length and time scales, in addition of having thermal fluctuations to replicate Brownian random motion[13]. Moreover, particle based methods are better suited for systems with complex geometries than continuum theories[14]. A DPD system, similar to MD, consists of a set of discrete particles, that interact with each other through pairwise forces. Newton's second law is used to compute the trajectories of each of the particles in the system. The forces include in addition to the thermostat forces mentioned above, a conservative force that sets the structure of the system. The traditional method of obtaining these forces is to match certain macroscopic flow properties. In addition, when using the DPD in a channel scenario, no systematic method exists to find a wall-fluid force that conserve the structure and dynamical properties in the confinement. Recently, efforts have been made to systematically find the different DPD forces using the mori-zwanzig formalism[15]. This method is very similar in spirit to dynamical force matching used also to match the structure and dynamics of the atomistic system[16]. Nevertheless, both of these methods are not suitable for scenarios where a wall-fluid interaction has to be defined as well.

In this work, a coarse-grained water transport model accounting for wall-fluid interactions will be developed. The model combines the structure preserving CG methods to obtain wall-fluid and fluid-fluid interaction potentials with the DPD thermostat to control the viscosity of the fluid. The novelty here will be to include the wall-fluid friction factor as an optimization target when obtaining the interaction potentials, which makes this model suitable for nano-fluidic transport.

The organization of this thesis will go as follows: In chapter 2, the developed

transport model will be explained with all the necessary history and background. Next, in chapter 3, the simulation details required to develop and test the model will be provided. The results of these simulations are shown later in chapter 4. Finally, a conclusion with future work suggestions is given in chapter 5.

CHAPTER 2

MOLECULAR DYNAMICS AND THE COARSE-GRAINED TRANSPORT MODEL

In this chapter, the focus is to explain how molecular dynamics simulations work, and how to develop the coarse-grained model of the all-atom system. Hence, first, a brief description of MD is provided to give the necessary background, where the important details of how the simulations are run and how to extract the important properties from the simulations are given. Next, the DPD thermostat will be introduced, since it is an integral part of the coarse-grained molecular dynamics(CGMD) simulations. Finally, the coarse-grained model is developed in detail, illustrating its target properties, its numerical form, and the optimization scheme to determine the necessary parameters.

2.1 Molecular Dynamics Simulations

Molecular dynamics(MD) is used to simulate matter at the atomic scale. Although atoms are not the smallest building blocks of matter, they are small enough to capture the important physical phenomena in many systems. One very important example is the structure and transport of fluids inside nano-channels, where classical continuum approximations fail to predict the behavior of the system. The atoms in solid and fluid systems are always moving or vibrating, even when no external force is applied on the system. The motion of these atoms is dictated by the inter-molecular forces that the atoms exert on each other. Therefore, to be able to predict the behavior of atomistic scale systems, a definition of the interaction potential between the particles

is required. The particle positions are then updated based on Newton's second law of motion. Starting from an initial configuration $\mathbf{r} = \{r_i, i \in [1, N]\}$, N being the number of particles in the system, the acceleration of individual atoms is determined through

$$a_i = \frac{F_i}{m} \tag{2.1}$$

where

$$F_i = \sum_{j \neq i}^{N} \frac{\partial U_{ij}(\|\vec{r_{ij}}\|)}{\partial r} e_{ij}$$

and $\vec{r_{ij}} = \vec{r_j} - \vec{r_i}$, $e_{ij} = \frac{\vec{r_{ij}}}{\|\vec{r_{ij}}\|}$, and U_{ij} is the interaction potential between particles i and j.

Boundary conditions are crucial while setting MD simulations. When simulating bulk material, the goal is to understand the behavior of the system atoms as if they are present in the interior of an infinite medium made of the exact same material. In that case, the behavior of the system is expected to be uniform throughout the defined system with no direction dependence. These simulations are used to study the behavior of systems away from interfaces, in the bulk of the material. Therefore to achieve this goal, periodic boundary conditions in all directions should be used. The system, in general, will be a 3D simulation box, with atoms located inside. If an atom leaves the box from one side, it will enter the system back from the opposite side. On the other hand, when a fluid is simulated inside nano-channel, all the bulk assumptions are not valid anymore. Choosing a boundary condition will depend on the nano-channel shape and size. In this work, only the 2D slit channel will be considered. In that case, the goal is to simulate the flow in an infinitely long and infinitely wide channel, but the height being fixed in the nano-meter range. Therefore, periodic boundary conditions will be applied in x and y-directions while in the z-direction the boundary is fixed, and the frozen wall atoms will stop the fluid molecules from exiting the system in the z-direction.

After defining the force-fields and boundary conditions, the simulation is run for

a specific number of time steps. At the beginning of each time step, the acceleration of each atom is calculated using equation 2.1. The velocity of each particle is determined from the previous state. Using the accelerations and velocities, different algorithms can be used to update the positions of the particles. Whatever the algorithm used, the time step determines how far a particle will move. Since the potentials have a hardcore part that induces a virtually infinite force when the particles become very close, a large time step can cause instability in the system through unrealistically placing atoms at a very close distance. Hence a very small time step of around 1fms is typically used. The small time step and heavy force calculations put a big limitation on the time scale of MD simulations. Usually, the simulation time is in the order of 10 nano-seconds for nano-meter scale systems having 1000-10000 atoms.

While running the simulations, important properties are dumped every specified number of time steps. These properties mainly include particle positions, velocities, and forces. All the other system properties can be derived from the three mentioned quantities, including temperature, pressure, and structure. Of particular importance to this work, the density of the fluid molecules, friction factor between wall and fluid, velocity profiles and bulk viscosity are of particular importance. Hence the calculation of these properties is explained in detail below.

2.1.1 Computing Density ρ

Since the bulk state is homogeneous and the system is uniform, density will be constant in the system. On the other hand, the presence of a wall in the system makes the density non-uniform the z-direction as shown in figure 2.1. The density will be computed as a function of the confinement coordinate z. First, the confinement will be split into equally sized bins with height $\Delta z = 0.5\sigma_{water} = 0.01585$ nm. Hence the

density in each bin will be determined as:

$$\rho(i) = (\frac{1}{N_{frames}}) \sum_{frame=1}^{N_{frames}} N(z_i, frame) \tag{2.2}$$

where $N(z_i, frame)$ is the number of particles having a z coordinate in the interval $[z_i, z_i + \Delta z]$ at a certain frame and $z_i = i * \Delta z$. The bin number i goes from 0 to $N_{bins} - 1$ and $N_{bins} = \frac{L_z}{\Delta z}$. Each frame represents a dumped state of the system during the simulation, and the density at in every bin will be averaged over all the frames.

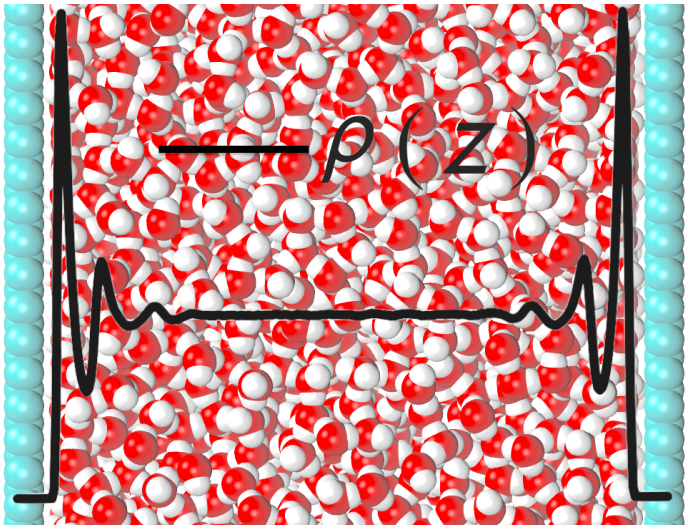

Figure 2.1: Illustration of the density layering in a graphene-water 2D slit nano-channel.

2.1.2 Computing Friction ζ

Velocity slip at the interface is a common phenomenon in nano-confined fluidic transport systems. The slip depends on two factors: operating conditions such as the driving force applied, and the friction factor with the interfacial wall.

The friction force at the interface is the result of multiple particles interacting with the walls in that region. The value of the friction factor will highly depend on the strength of the wall-fluid force and the structure of the wall atoms [17]. Since the wall is discrete, the potential that the fluid atoms feel depends on the position parallel to the wall. Hence there will be potential wells present in the region for the fluid atoms. A smooth wall whose interaction with the fluid does not change much in the direction parallel to the wall, provide less resistance to fluid motion compared to a corrugated wall that will tend to increase the friction in the system.

Calculating the friction factor is done using a Green-Kubo approximation. The relation derived by Huang et. al. in ref[18], computes the friction factor as follows.

$$\zeta_j = \frac{< \int_0^\infty f_{x,j}^{wf}(0) f_{x,j}^{wf}(t) dt >}{k_B T + < \int_0^\infty f_{x,j}^{wf}(0) v_{x,j}^{wf}(t) dt >} \tag{2.3}$$

where ζ_j is the friction coefficient of particle j. $f_{x,j}^{wf}$ and $v_{x,j}^{wf}$ are the wall-fluid force and velocity in the streaming direction of particle j. The integrands in the numerator and the denominator are the force auto-correlation function(FACF) and the force-velocity auto-correlation function(FVACF). The bracket symbol $< ... >$ resembles taking an ensemble average. Both of the integrals will be computed numerically using data dumped at every 10 fs. This dumping time step is usually small enough to give accurate values. Finally, the total friction factor between fluid and interface is

$$\zeta = \sum_j^N \zeta_j \tag{2.4}$$

where N is the total number of particles in the interfacial region. The interfacial region is defined by $z > L_z - \delta$ and $z < \delta$. Therefore as δ is increased, more particles will be in that interfacial region, and hence ζ will increase. Nevertheless, there exists a δ_{max} after which the friction factor ζ does not increase significantly. To determine δ_{max}, $zeta$ is computed using increasing values of δ starting from $\delta = 0$ nm.The distance δ at which the friction factor reaches a constant value as a function of δ is

equal to δ_{max}. When computing *zeta* in the CG system, the same δ_{max} will be used for consistency.

2.1.3 Viscosity μ

The viscosity of a fluid is one of the key properties that determine its transport behavior. Since computing the property in the confined inhomogenious system is not well established, the viscosity calculation will be done for the bulk system. After running a bulk simulation for the considered fluid, the dumped pressure tensor will be used to compute viscosity compute it using the Green-Kubo relation[19]:

$$\mu = \frac{V}{K_B T} \int_0^\infty \frac{1}{6} \sum_\alpha \sum_{\beta \neq \alpha} P_{\alpha\beta}(0) P_{\alpha\beta}(t) dt \tag{2.5}$$

where α and β are directions in the Cartesian coordinates(x,y,z), V is the volume of the system, and $P_{\alpha\beta}$ is the $\alpha\beta$ component in the pressure tensor. The integrand in equation 2.16 is the pressure auto-correlation function (PACF). Again this integral is computed numerically. The off-diagonal pressure components are dumped and stored every 1 fs.

2.2 The DPD Thermostat

Simulating system in an isothermal state requires the use of a thermostat. The algorithm briefly described above for MD simulations assume an NVE ensemble where the temperature is allowed to change. For an NVT ensemble that fixes the number of particles N, volume V and temperature T, a thermostat has to be used. The thermostat adjusts the velocities of the atoms at each time step such that the temperature is preserved while the total energy in the system is allowed to change. The typical thermostat commonly used for MD simulations is the NoseHoover thermostat(NH)[20].

The NH thermostat does not affect the viscosity or diffusion of the system. Hence when researchers want to slow down the dynamics of CG systems as explained in chapter 1, a different thermostat is used. A very common choice that will be used in this work is the dissipative particle dynamics(DPD) thermostat. Dissipative particle dynamics was first developed by Hogelburge and Koleman in 1991[13]. The goal was to have an efficient particle based method that is able to simulate the correct hydrodynamic behavior over a large length and time scales, in addition of having thermal fluctuations able to replicate Brownian random motion. Moreover, particle-based methods are better suited for complex geometries compared to continuum methods. [14]

The algorithm adds additional pairwise forces compared to MD simulations ran using the NH thermostat. The total force acting on a particle i at a certain time step is computed as the sum of the inter-particle forces between particle i and the rest of the $N-1$ particles in the system as:

$$F_i = \sum_{j \neq i} F_{ij}^C(\vec{r_{ij}}) + F_{ij}^D(\vec{r_{ij}}, \vec{v_{ij}}) + F_{ij}^R(\vec{r_{ij}}) \tag{2.6}$$

where F^C is the conservative force, F^D is the dissipative force, and F^R is the random force.

In MD simulations using NH thermostat, only the conservative force F_{ij}^C is included, where it is derived from the pair potential between atom i and atom j. The potentials usually have a highly repulsive core such as the Lennard-Jones(LJ) 12-6 potential[21]. This forces the time step dt to be very small(order of a fs). In DPD the conservative force is also derived from a potential. However, given that particles i and j are pseudo-particles that do not correspond to a realistic physical structure, there is no restriction on this potential, as long as it conserves the hydrodynamics. The condition for that is simply that the inter-particle forces are equal and opposite. Since this condition forces the conservation of momentum in the system, correct hydrodynamics are automatically replicated[22]. Hence a simple soft core potential is usually used to derive the conservative force in DPD. The oldest and most famous

form is

$$F_{ij}^{C}(\vec{r_{ij}}) = \alpha_{ij}(1 - \frac{|\vec{r_{ij}}|}{r_{cut}})\vec{e_{ij}} \tag{2.7}$$

where r_{cut} is the cutoff distance of the pairwise interaction. Using this form, a relatively large time step can be used, which will allow for a longer simulation time. The dissipative force is given as:

$$F_{ij}^{D}(\vec{r_{ij}}, \vec{v_{ij}}) = -\gamma_{ij}\omega^{D}(\vec{r_{ij}})(\vec{e_{ij}}.\vec{v_{ij}})\vec{e_{ij}} \tag{2.8}$$

where $\vec{v_{ij}} = \vec{v_j} - \vec{v_i}$ is the velocity difference vector between particle i and j. This force is proportional to the velocity difference between particles i and j, and act along the line joining the centers of these particles in the direction opposite to the velocity gradient. Hence it will act as a friction force that will decrease the velocity difference between the particles producing a 'viscous' effect in the system. The strength of this force is controlled through its coefficient γ_{ij}. In addition, the dissipative force has an inter-particle distance dependence specified by $\omega^{D}(\vec{r_{ij}})$. The basic functional form of the dissipative form coefficient is $\omega^{D}(\vec{r_{ij}}) = (1 - \frac{|\vec{r_{ij}}|}{r_{cut}})^2$. In recent works, the power of 2 in this functional form is changed to improve the force matching between MD and DPD[15].In this work, the traditional form will be used due to ease of implementation using commercial packages.

The random force takes the following form:

$$F_{ij}^{R}(\vec{r_{ij}}) = \sigma_{ij}\omega^{R}(\vec{r_{ij}})\zeta_{ij}\Delta t^{-1/2}\vec{e_{ij}} \tag{2.9}$$

The randomness of this force is due to ζ_{ij} which is a random variable generated from a Gaussian distribution with zero mean and unit variance. σ_{ij} determines the strength of this force, and $\omega^{R}(\vec{r_{ij}})$ controls the distance dependence. The first DPD scheme proposed did not properly sample the canonical NVT ensemble. This is because the fluctuation-dissipation theorem was not enforced. It was until 1995 when Espanol and Warren derived the following constraints on the parameter space that will ensure

that fluctuation dissipation theorem will be satisfied[23]:

$$\sigma^2 = 2\gamma kT \tag{2.10}$$

$$\omega^D = [\omega^R]^2 \tag{2.11}$$

DPD can be used in AAMD or CGMD simulations as just a thermostat. In that case, the F_{ij}^C will be replaced by the AAMD or CGMD potentials, keeping the dissipative and random forces the same. This will ensure that the temperature of the system is fixed a a set temperature, in addition to slowing the dynamics of the system.

2.3 The Coarse-Grained Transport Model

The main objective of this work is to develop a coarse-grained transport model for fluid molecules inside nano-channels. By coarse-graining an atomistic system, the computational resources required to run the MD simulations will be less. The decrease in simulation time opens the door for simulating new phenomena efficiently. A coarse-graining procedure is divided into four main steps. First, a mapping between the all-atom AAMD system and CGMD system should be developed. Since the choice of mapping the fluid molecules highly depends on the studied system, little focus will be given to this step. Briefly, in the case of water being the fluid, each water molecule will be represented by one atom, instead of one oxygen and two hydrogen atoms. The mapped system when simulated should match certain properties of the MD system. Defining these target properties is the second step of developing the CG model. Having the targets in mind, the functional form of the interaction potential between the different types of particles will be determined in the third step of the process. Finally, an optimization scheme should be devised to obtain the potential parameters which specifically math the target properties of the system of interest. To demonstrate the ability of the model in replicating structural and dynamical properties in the confinement, it will be applied to the water-graphene

system. To simplify the task at hand, we are going to restrict ourselves to the NVT ensemble at a constant temperature of 300K. In addition, we are going to use a slit shaped 2D nano-channel to develop and verify our model. Figure 2.2 shows a sample explicit water-graphene system, alongside the mapped CG system of the same size. Although the slit geometry is simple, it includes all the important aspects of transport: slip at the wall, viscous stresses, and wall-fluid layering. The choice of water as the fluid is due its importance from the scientific and practical point of view. The flow of water is critical in many biological and chemical systems. In particular, the water-graphene combination has been suggested previously for fast transport of water in many applications. Hence developing a coarse-grained model for this system will pave the way for developing coarse-grained models for other combinations of fluids and nano-channel walls.

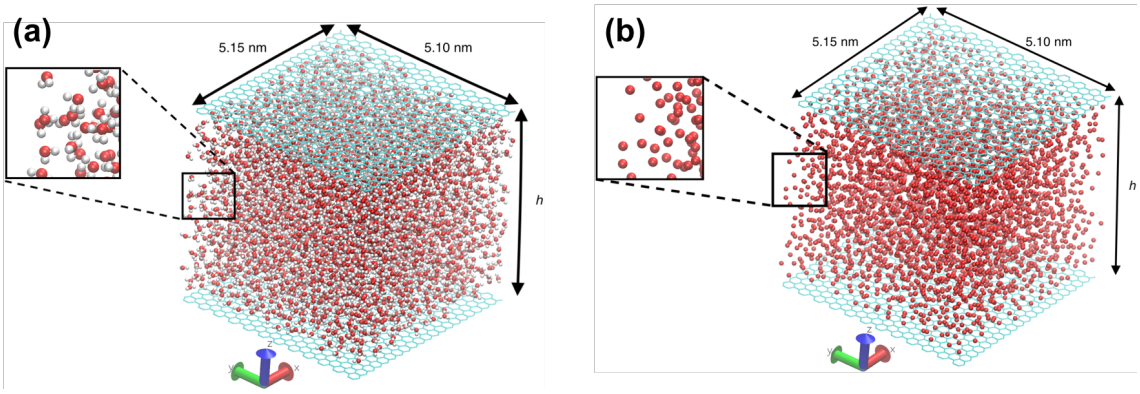

Figure 2.2: Illustration of mapping the water-graphene system from the full atomistic representation(a) to the coarse-grained representation(b).

2.3.1 The Target Properties of The CG Model

The coarse-grained model developed should accurately match the transport behavior simulated by MD. By matching the transport behavior, we mean that the steady-state velocity profile of the CG model should quantitatively agree with the velocity

profile obtained from all-atom MD under different driving conditions. Ideally, this model should also be transferable for different geometric shapes and sizes. The non-equilibrium simulations needed to obtain the velocity profiles are very expensive in nature. Hence setting the velocity profile as a direct optimization target is not a feasible option, since the objective function will include the velocity profile at different flow conditions. Therefore, the direct optimization target should be relevant equilibrium properties that are less expensive to compute.

Classical hydrodynamic behavior is well described by the Navier-Stokes conservation equations. Many researchers tried to use continuum methods to predict transport in simple nano-fluidic geometries such as slits and cylindrical nanotubes[24]. Specific adjustments were made to the continuum models in order to match transport behaviour. First, we know that in nano-channels, velocity slip at the walls occurs in many systems. In addition, density in the confinement is not constant which needs to be included in the conservation of momentum equation. The density variation gives rise to viscosity changes as well, which also needs to be incorporated in the equations for accurate transport prediction. Based on this, the three target properties for the CG model will be the density profile, wall fluid friction factor, and bulk viscosity.

2.3.2 The Model Parameters

The CG model is expected to match the target properties of the AAMD system. Computing the properties for the CG model requires running a CG molecular dynamics(CGMD) simulation. The results of the simulations will depend on the interaction potentials and the parameters that determine them. Below a detailed description of the interaction potentials and the used thermostat will be provided. The force in the developed model is computed as specified in equation 2.5. The system consists of fluid CG particles and wall atoms. Fluid CG particles will be referred to as 'CG', and wall particles as 'W'. The conservative force on a CG particle i imparted by

particle j will be given as:

$$F_{ij}^{C}(\vec{r_{ij}}) = \frac{\partial U_{ij}(\|\vec{r_{ij}}\|)}{\partial r}\vec{e_{ij}} \tag{2.12}$$

Where

$$U_{ij}(r) = \begin{cases} U(p_f, r) & \text{if } j \text{ is a fluid CG particle} \\ U(p_w, r) & \text{if } j \text{ is a wall particle} \end{cases} \tag{2.13}$$

p_f and p_w are the parameter sets for the interaction between CG particles and between CG particles and wall particles respectively. In recent works, a versatile spline potential was used for the structure matching CG problems allowing for a larger sample space[25]. Nevertheless here the modified Lennard-Jones Gaussian potential form is used, which has fewer parameters to optimize for simplicity[26]. The potential is defined as:

$$U(p, r) = \begin{cases} U_{CKD}(r) + le^{\frac{-(r-t)^2}{2s^2}} - le^{\frac{-(r_c-t)^2}{2s^2}} & r < r_{cut} \\ 0 & r \geq r_{cut} \end{cases} \tag{2.14}$$

where

$$U_{CKD}(r) = \begin{cases} 4\epsilon((\frac{\sigma}{r})^{12} - (\frac{\sigma}{r})^6 + \frac{1}{4}) & r < r_{c,LJ} \\ -\epsilon(cos^2(\frac{\pi(r-r_{c,LJ})}{2w_c})) & r_{c,LJ} < r < r_{c,LJ} + w_c \\ 0 & r_{c,LJ} + w_c < r \end{cases}$$

and

$$r_{c,LJ} = \sigma 2^{1/6}$$

and

$$p = [\sigma, \epsilon, w_c, l, t, s]$$

The parameters σ and ϵ are the normal length and energy scales of the LJ potential. w_c is a smoothness parameter for the attractive part of the potential. l, t, and s are the Gaussian parameters. Therefore there are 6 free parameters in this potential: σ, ϵ, w_c, l, t, and s. The units of energy and distance are KJ/mol and nm respectively.

The thermostat used for the CGMD simulations is the DPD thermostat. The DPD thermostat provides the versatility of tuning the viscosity of the fluid. For the dissipative force computation, equations 2.8 and 2.9 will be invoked. This force will only exist between the fluid particles. The results later will show that the wall-fluid dynamics can be set to match target AAMD dynamics without the need of a dissipative force. Trying to coarse-grian the system with the simplest possible model, no dissipative force exists between the wall and CG particles, and therefore:

$$F_{ij}^{D}(\vec{r_{ij}}, \vec{v_{ij}}) = \begin{cases} -\gamma(1 - \frac{\|\vec{r_{ij}}\|}{r_{cut}}^2(\vec{e_{ij}}.\vec{v_{ij}})\vec{e_{ij}} & \text{if } j \text{ is a water CG particle} \\ 0 & \text{if } j \text{ is a wall particle} \end{cases} \tag{2.15}$$

And Similarly for the random force:

$$F_{ij}^{R}(\vec{r_{ij}}) = \begin{cases} \sqrt{2\gamma kT}(1 - \frac{\|\vec{r_{ij}}\|}{r_{cut}})\zeta_{ij}\Delta t^{-1/2}\vec{e_{ij}} & \text{if } j \text{ is a water CG particle} \\ 0 & \text{if } j \text{ is a wall particle} \end{cases} \tag{2.16}$$

Hence, this model has thirteen parameters to optimize, twelve for the conservative potentials and one for the thermostat. Namely, the parameters to optimize are $p_f = [\sigma_f, \epsilon_f, w_{c,f}, l_f, t_f, s_f]$, $p_w = [\sigma_w, \epsilon_w, w_{c,w}, l_w, t_w, s_w]$, and γ.

2.3.3 Optimization Scheme

After formulating the model, we need to set its free parameters to match the properties of interest of the MD system. The ensemble considered is the canonical NVT ensemble. T will be fixed at 300K for all the simulations done in this work. The cutoff distance r_{cut} is chosen to be 1.2nm, which is a safe choice given that the conservative potentials will become negligible at a smaller inter-particle distance. The properties of interest to be matched are divided into two categories: bulk fluid-specific properties and wall-fluid properties. The first category includes the viscosity of the bulk fluid and the second one include the wall-fluid friction factor ζ and the fluid

confinement density profile $\rho(z)$. Since the wall-fluid properties depend on the confinement height, the optimization will be done at a specific height. For example, for the water-graphene system that will be considered here, the optimization will take place in a $15\sigma = 15 \times 0.317 = 4.755nm$ channel. Later the results will be verified for different channel sizes.

The parameters p_w, p_w, and γ each affect the target properties of the CGMD system differently. The structure and friction coefficients depend on all the potential parameters p_f and p_w. Although the dissipative force coefficient γ does not affect the structure, the friction coefficient linearly depends on it as was found from the CGMD simulations. The bulk viscosity only depends on p_f and γ, since in bulk simulations the interaction between CG and W is absent. Moreover, the density profile and friction coefficient are wall-fluid properties that require confinement equilibrium simulations to be computed, while the bulk viscosity is computed from bulk simulations only. Based on how each parameter affects the target properties and the simulation type it requires, obtaining the optimal parameter set is divided into three steps. The strategy described here is not unique, but it was found the fastest route to reach the optimal set of parameters.

In step I, p_f^I and p_w^I will be found through matching the density profile of water in the confinement system. This means that the potentials $\mathbf{U^I} = U(p_f^I, r), U(p_w^I, r)$ will be updated in iterations until a satisfactory match between the confinement CGMD density profile and AAMD density profile is reached. The DPD thermostat will not be used, reflecting a case of $\gamma = 0$ and the temperature is set through the Nose-Hoover thermostat. Formally we want to minimize the error between the two equilibrium density profiles in the confinement defined as:

$$y_1 = [\sum_{i}^{z=z_{max}} |\rho_{CGMD}(i) - \rho_{AAMD}(i)|] = E_\rho \tag{2.17}$$

The optimization to reach the minimum is done using the downhill simplex algorithm. Simplex is a gradient-free method, which allows for versatility in defining the minimization target[25]. Simplex from $n+1$ set of initial points where n is the number of parameters. Based on the objective function value for each point, it updates its parameter set to find the objective function at the newly added points. Given the nonlinearity of the problem and the heuristic method used, convergence may not be possible if the initial parameter set is not good enough. Adding to the difficulty is the fact that evaluating y_1 requires running a CGMD simulation using the updated set of potentials $\mathbf{U^I}$. Nevertheless, the simulation time required to compute the density is around three times less than that required to compute friction factor in the confinement. Therefore the friction factor is not included in the objective of this step, which will allow us to run more iterations to find a point that matches density, which will be a better starting point for friction+density optimization steps later. At the end of the step, around 10 bulk simulations, with different γ values combined the optimized p_f^I, will be done to determine the value of γ^I that matched bulk viscosity. Therefore in step II below, the Nose-hoover thermostat will be replaced with the DPD thermostat with the value γ^I for the dissipative force coefficient that was found to match bulk viscosity.

After obtaining $\mathbf{U^I}$, $\mathbf{U^{II}}$ will be found by adding the error in the friction factor ζ to the error function. Therefore

$$y_2 = [\sum_{i}^{z=z_{max}} |\rho_{CGMD}(i) - \rho_{AAMD}(i)|] + a(|\zeta_{CGMD} - \zeta_{AAMD}|) = E_\rho + aE_\zeta \quad (2.18)$$

where E_ρ and E_ζ are the root-mean-squared error in density ρ and friction ζ, and a is a weighting coefficient. In this step, we fix σ, ϵ, and w_c to the values obtained for $\mathbf{U^I}$, and allow only l, t and s to vary. Therefore this optimization will have a total of 6 parameters to optimize. This makes the optimization process faster and keeps the solution close to the structure matched solution. The reason we divided the first two steps, is to reduce the number of parameters when minimizing $|\zeta_{CGMD} - \zeta_{AAMD}|$. The simulations done in step two are run for longer time, to be able to compute ζ

from them. Hence minimizing the number of required iterations by decreasing the number of optimized parameters is necessary. At the end of this step, again a new value of γ has to be found since now a new set of fluid-fluid potential p_f^{II} was found. As a result, the friction factor may be slightly changed. Hence we need a final step, where we fix γ to γ^{II} and p_f^{III} to p_f^{II} and vary only p_w. Exceptionally, if the change in friction factor, after γ is optimized in step II, is not significant then step III will not be needed. Figure 2.3 summarizes the different steps of the optimization scheme.

The fact that this model is using fitting parameters does not make it ad-hoc. As will be shown later, once the fitting parameters are found for one system, they enjoy generality for different channel widths and driving forces. This is a merit of the fact that the parameters are found by matching key microscopic physical properties that determine the structure and the dynamics of the system. The optimization scheme described here is not unique, but was found to be the most efficient given the high computational cost of MD simulations.

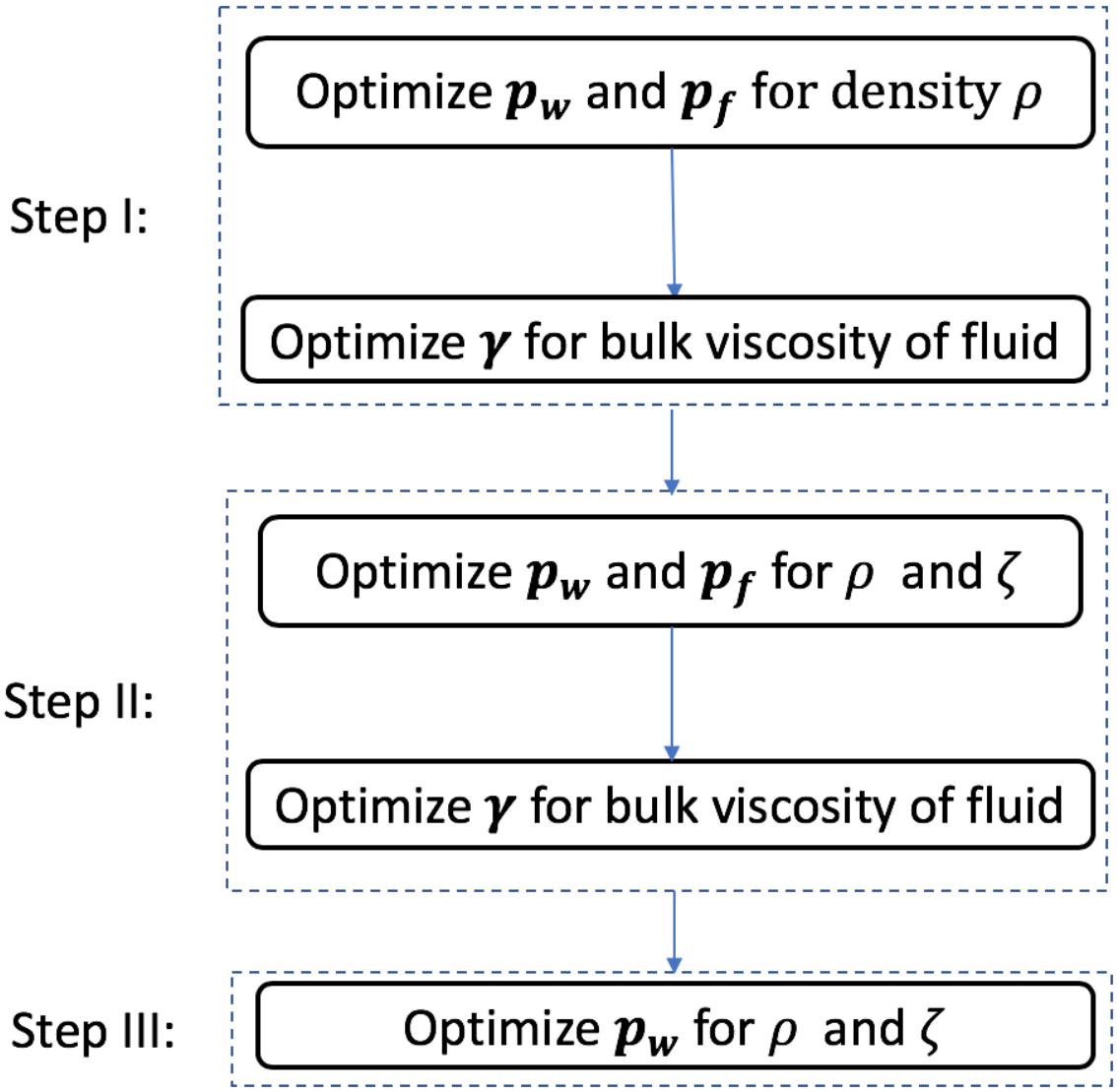

Figure 2.3: Illustration of the optimization scheme used to determine the model parameters.

CHAPTER 3

METHODS AND SIMULATION DETAILS

After developing the CG model and the outlining the procedure needed to determine its free parameters, the numerical details of the necessary simulations will be provided in this chapter. First, in section 3.1, the simulation details of the fine-grained all-atom molecular dynamics system are provided. Next section 3.2, discusses the difference in simulating the AAMD and coarse-grained system. Finally, section 3.3 talks about running the optimization using the VOTCA package which was developed to optimize potentials of CG simulations.

3.1 All-atom Molecular Dynamics Simulations

The transport system that will be studied in this work is a rectangular 2 dimensional(2D) Graphene channel. Although the slit geometry is simple, it includes all the important aspects of transport: slip at the wall, viscous stresses, and wall-fluid layering. Moreover, Graphene has emerged as a very interesting material to drive water at high speeds. Hence, the channel walls used in this work are single-layered hexagonal graphene. As shown in figure 3.1, the lateral dimensions of the graphene sheets are 5.15x5.10nm with a height h, which will be in the range of 3-7nm. As mentioned earlier the fluid in the channel is explicit water.

The NVT ensemble is used to carry the simulations. The volume is fixed a priory by the box dimensions and T is fixed at 300K. The number of particles is chosen

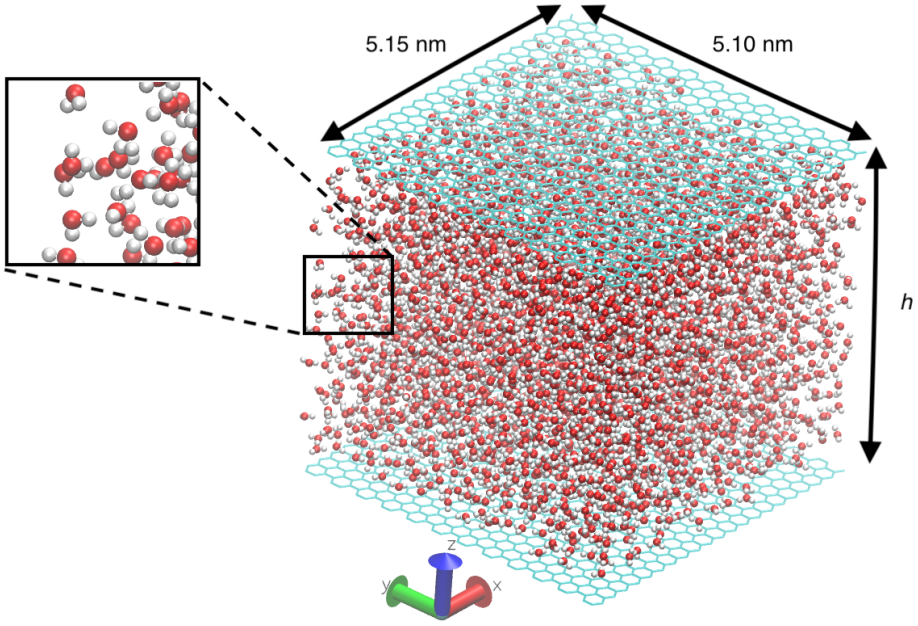

Figure 3.1: All-atom molecular dynamics system initial configuration. Carbon hexagonal Graphene atoms are shown in blue, while water molecules colored with red(Oxygen) and white(Hydrogen).

such that the water in the confinement is at equilibrium with bulk water at a pressure of 1 bar and temperature of 300K. The number is determined through the method described in reference [27], through which we add or remove particles from the confinement system until the bulk region in the channel has a density equal to 33.46 nm^{-3} which is the density of water at 1 bar and 300K.

All the MD simulations are run using LAMMPS. The water model used for the all-atom simulations is the extended simple point charge(SPC/E) model[28]. The LJ 12-6 interaction is used between the carbon and oxygen atoms. The σ and ϵ of the oxygen-oxygen(OO) and carbon-carbon(CC) are given in table 3.1. The arithmetic mixing rule available in LAMMPS was used to derive the other LJ interaction parameters. The cutoff of all the LJ interactions is set at 1.2nm. Electrostatic interactions are computed using a particle Mesh Ewald (PME) method[29]. A vacuum space is placed in the z-direction to isolate the top and bottom parts of the confinement. Periodic boundary conditions are used in the x and y directions. The wall atoms are fixed in their initial positions during the simulations. The NH thermostat is used to fix the temperature at 300K. The time step of the simulations is 1 fs.
A constant force is used to transport the fluid in the non-equilibrium simulations. This is done by applying a constant force in the x-direction on each particle. Given that the thermostat computes the temperature based on the velocity of the fluid, only the z and y-direction speeds will be used in the temperature calculations. Non-equilibrium simulations are run in 5 batches each for 10ns after 2ns of equilibration unless otherwise specified. The particle velocities and positions are dumped every 20 fs.

Table 3.1: LJ interaction parameters for the AAMD simulations

σ_{CC}(nm)	σ_{OO}(nm)	ϵ_{CC}(KJ/mol)	ϵ_{OO}(KJ/mol)	r_{cut}(nm)
0.3390	0.3165	0.233	0.6503	1.2

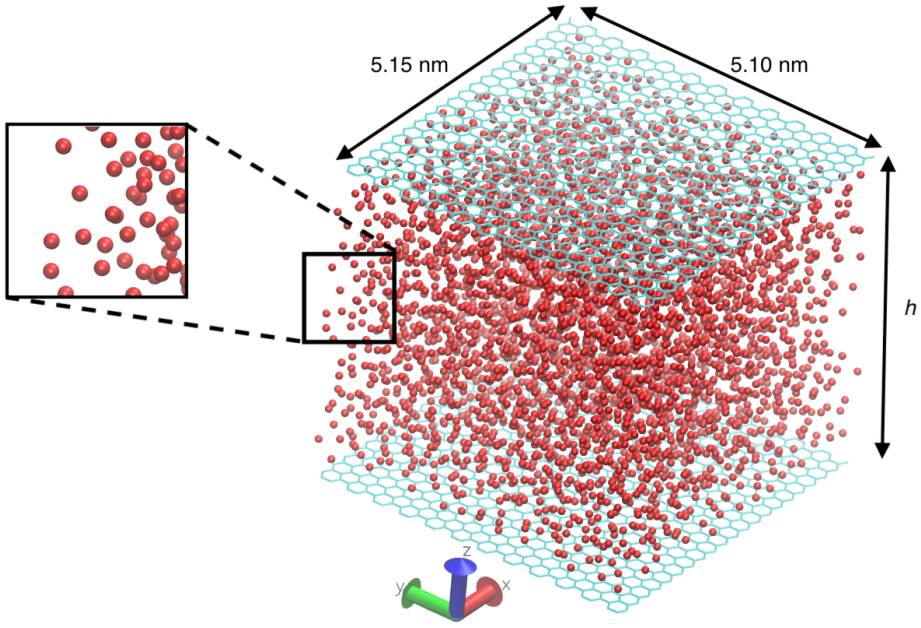

Figure 3.2: Coarse-grained system initial configuration. Carbon hexagonal graphene atoms are shown in blue, while water CG particles colored with red.

3.2 Coarse-grained Simulations

The CG simulations are performed to develop and test the CG transport model. The confinement system is identical to the AAMD system described above, except that the explicit water molecule will be replaced with a CG water molecule as shown in figure 3.2. The number of CG water molecules in the confinement is equal to the number determined for the AAMD system. The conservative interaction between the particles, and between the particles and the wall is given through tabulated potentials generated using the modified LJ potential described in chapter 2. We use the DPD force field available in LAMMPS with specifying the γ, r_{cut} and T. The DPD conservative force is set to zero because it is replaced by the tabulated potentials, which is overlayed on the DPD potential. The DPD force acts as a thermostat. Therefore no additional thermostat will be used.

In addition to the confinement simulations, bulk simulations are needed to optimize

for bulk viscosity. The dissipative force magnitude γ of the model is determined by matching the bulk viscosity of the coarse-grained water, with the bulk viscosity of water. Therefore bulk simulations of both the CG system were performed to obtain their viscosity and determine the γ value that matches the viscosity of SPC/E water. The bulk CGMD simulations will only differ from the confinement CGMD simulations through the fact that no wall molecules are present. Simulations are run for 5ns, where the pressure tensor is output every 1 fs. This ensures for that the integral in equation 2.5 converges accurately.

3.3 CG Model Optimization

VOTCA is a package developed to generate coarse-grained potentials[30], that are able to match the structure and thermodynamic properties of a target all-atom molecular dynamics system. Many coarse-graining methods are available for use with VOTCA. In this work, we will use the downhill simplex optimizer to obtain our coarse-grained potentials. Since simplex is a gradient-free method, it will allow us to easily incorporate the friction factor between water and the walls into the objective function.

During the optimization procedure, the potential is iteratively updated, until a satisfactory match is found for the target properties. In each iteration, the objective function is evaluated by running a CG simulation and post-processing it to extract the properties of interest. These are then compared to the target values obtained from the AAMD simulations, and a suitable update is made on the potential parameters. The target quantities of the AAMD system are obtained by running equilibrium simulations in bulk and confinement for 10ns each. The CG simulations are ran for 1.5ns during the objective function evaluation that involves the calculation of friction factor. On the other hand, when the objective function only includes the error in density, it is enough to run the CG simulations for 750 ps to extract a well-converged

density estimate. Finally, since the VOTCA package does not support optimization for friction factor, computing friction was added to the package by implementing the method outlined in section 2.5.2.

CHAPTER 4

RESULTS

In this chapter, the results of applying the developed CG model on the Water-Graphene system are shown. First, the success of the optimization scheme is demonstrated, showing an excellent match with the AAMD system in all the set target properties. Moreover, the results of the non-equilibrium transport in the CG system will be compared to the AAMD results to test the performance of the developed model.

4.1 Optimization Scheme

The goal of the optimization scheme is to obtain the model parameters at which the CGMD model matches the key properties of the AAMD system. Following the strategy outlined in section 2.4, a great match was obtained in all the different properties. The error in the density profile was less than 7%, and that can be seen from the great match in figure 4.1. An exact match was possible for bulk viscosity and an error of less than 1% for friction coefficient, as shown in table 4.1 below.

Table 4.1: Comparison of optimization targets ζ and μ at the end of each phase with AAMD values

Parameter		**AAMD**	**CG**
Friction factor	$\zeta(\frac{\text{KJ.ps}}{\text{mol.nm}^2})$	16.18	16.23
Viscosity	μ(cP)	0.601	0.599

Figure 4.1: Density ρ profile comparison between the all-atom system and CG system after the final optimization step.

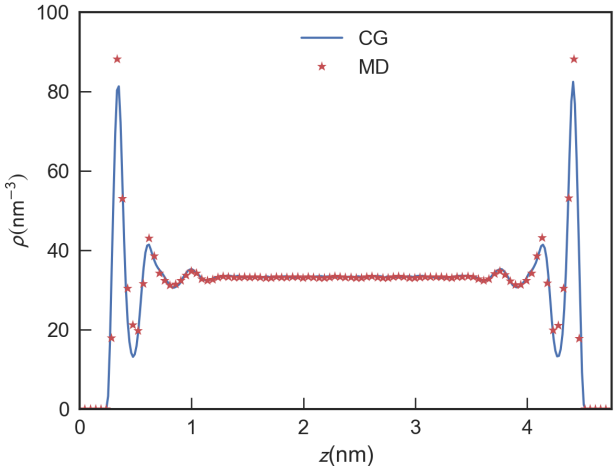

The downhill simplex algorithm convergence was good considering the highly non-linear nature of the objective function. The algorithm starts from a set of initial points and then replaces the worst one with a linear combination of the other points. It then keeps on updating the list of points it is considering based on the function value at each one. In figure 4.2, the plot shows the minimum value of the objective function as a function of the simplex iteration. Since not all the iterations will introduce a more optimal set, the plot of y_1 as a function of simplex iteration is varying discontinuously. The error in density in step I decreases from around 9% to around 6.5% in 150 iterations. The initial error value was acceptable, which means that the choice of initial parameters was good. Some of the initial parameter sets introduced high errors of 30%, but they do not appear in the plot since we are always showing the minimum error value at a certain iteration. Nevertheless, although quantitatively the error does not appear to decrease significantly, fine details in the density profiles were vastly improved. These changes occur specifically at the peaks of the plot, which will not contribute greatly to the error. After determining p_w^I and p_f^I through the simplex optimization, γ^I is found by running bulk simulations to

compute bulk viscosity. The results came such that $\gamma^I = 26$KJ/mol.nm would match the viscosity of the AAMD system. Using this γ value, step II attempts to minimize y_2. Since the density starts from its optimal solution point, and the weight of density error is higher in the objective function y_2, in figure 4.3 the error decreases slightly from around 8% to 6%. The error in ζ decreased from around 15% to around 0.3% at the end of the simplex optimization of step II. The interaction potential between CG particles did not change significantly between the two steps, causing the value of γ that matches the viscosity to stay at around 26.0 KJ/mol.nm. Therefore, step III was not needed in for this system. In total, 300ns of simulation time was needed to obtain the CG model parameters.

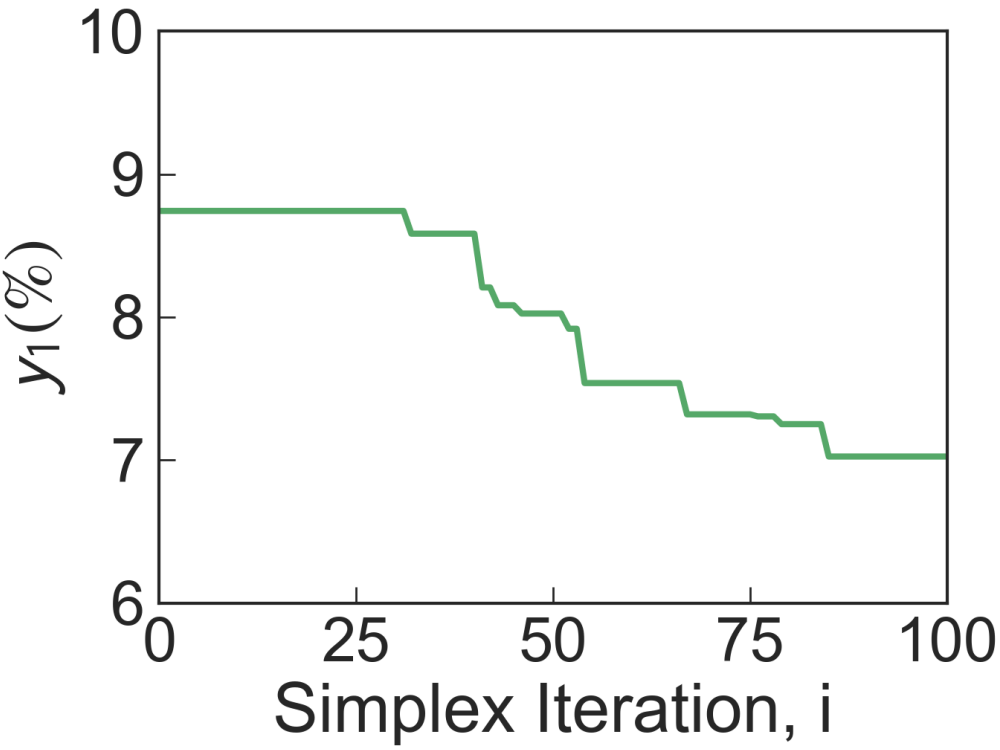

Figure 4.2: The convergence of the objective function y_1 for step I of the optimization scheme.

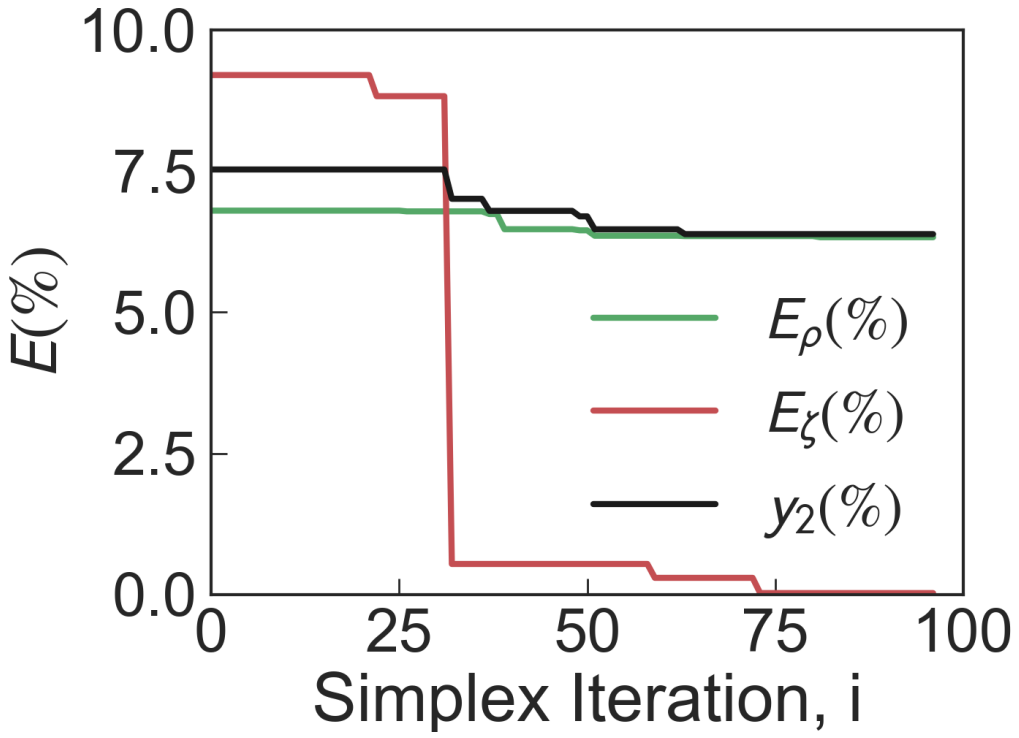

Figure 4.3: The convergence of the objective function y_2 for step I of the optimization scheme. The individual relative errors in density E_ρ and in friction E_ζ are also shown.

The potential form used in the model definition proved to be sufficient to match the desired properties. The interaction between CG molecules shown in figure 4.4, had the double well feature reported in previous work for the interaction between CG water single beads[26]. Table 4.2 lists the potential parameters at the end of each step. It can be observed how the parameters only changed slightly after step I and this is reflected in the slight change in the potential plot in figure 4.4 and figure 4.5. On the other hand, the interaction between W and CG molecules was closer to a pure LJ interaction as figure 4.5 shows. The pure LJ form was not forced, but rather was a result of the optimization procedure. The plot shows that also in this case the potentials did not change much after the density matching step. Nevertheless, the slight change in the potentials allowed the friction factor to change and match the

AAMD value. The final potential parameters, found in table 4.2, will be used to run the non-equilibrium flow simulations in the next section.

Table 4.2: The CG model parameters after step I and II.

	p_w						p_f						
Step	σ (nm)	ϵ ($\frac{\text{KJ}}{\text{mol}}$)	w_c (nm)	l ($\frac{\text{KJ}}{\text{mol}}$)	t (nm)	s (nm)	σ (nm)	ϵ ($\frac{\text{KJ}}{\text{mol}}$)	w_c (nm)	l ($\frac{\text{KJ}}{\text{mol}}$)	t (nm)	s (nm)	γ ($\frac{\text{KJ}}{\text{mol.nm}}$)
I	0.265	3.000	0.243	4.938	0.263	0.091	0.261	3.511	0.265	5.291	0.316	0.054	25.5
II	0.265	3.000	0.243	5.234	0.253	0.095	0.261	3.511	0.265	5.322	0.320	0.057	26.0

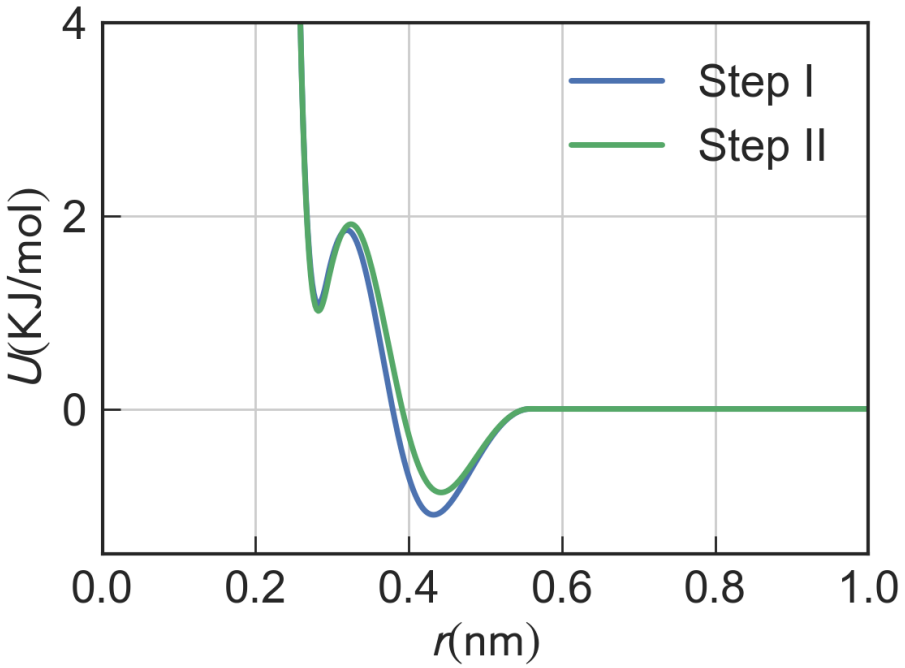

Figure 4.4: Modified LJ potentials of the CG-CG interaction after step I and II

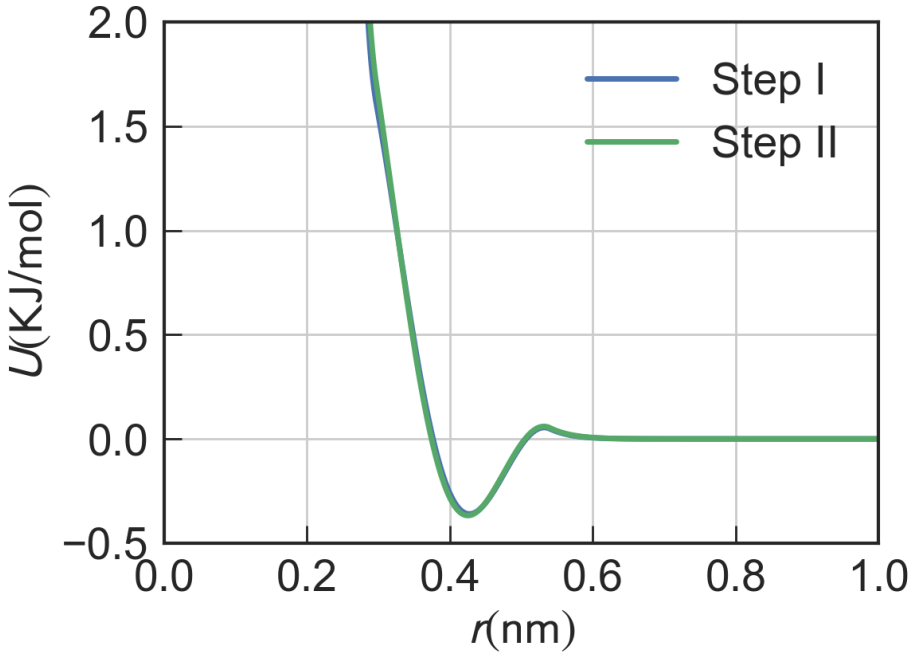

Figure 4.5: Modified LJ potentials of the W-CG interaction after step I and II

4.2 Non-equilibrium Simulations

After obtaining a CG model that can replicate the key transport properties, non-equilibrium CGMD and AAMD simulations were run to compare the transport behavior of the two systems. More precisely, Poiseuille flow will be simulated in the same slit system used for optimizing the model. The flow will be simulated in three different channels that vary by the height which will be set to 10σ, 15σ(where the model was optimized) 20σ. The diameter of the water molecule is estimated to be $\sigma = 0.317nm$. The Poiseuille-like flow is simulated by applying a constant acceleration g to the system. The equivalent pressure gradient in a poissoille flow is $\frac{dp}{dx} = \rho g$. Figure 4.6 shows the velocity and density profile of the flow in a 15 σ channel at $g = 0.1$J/mol.nm.

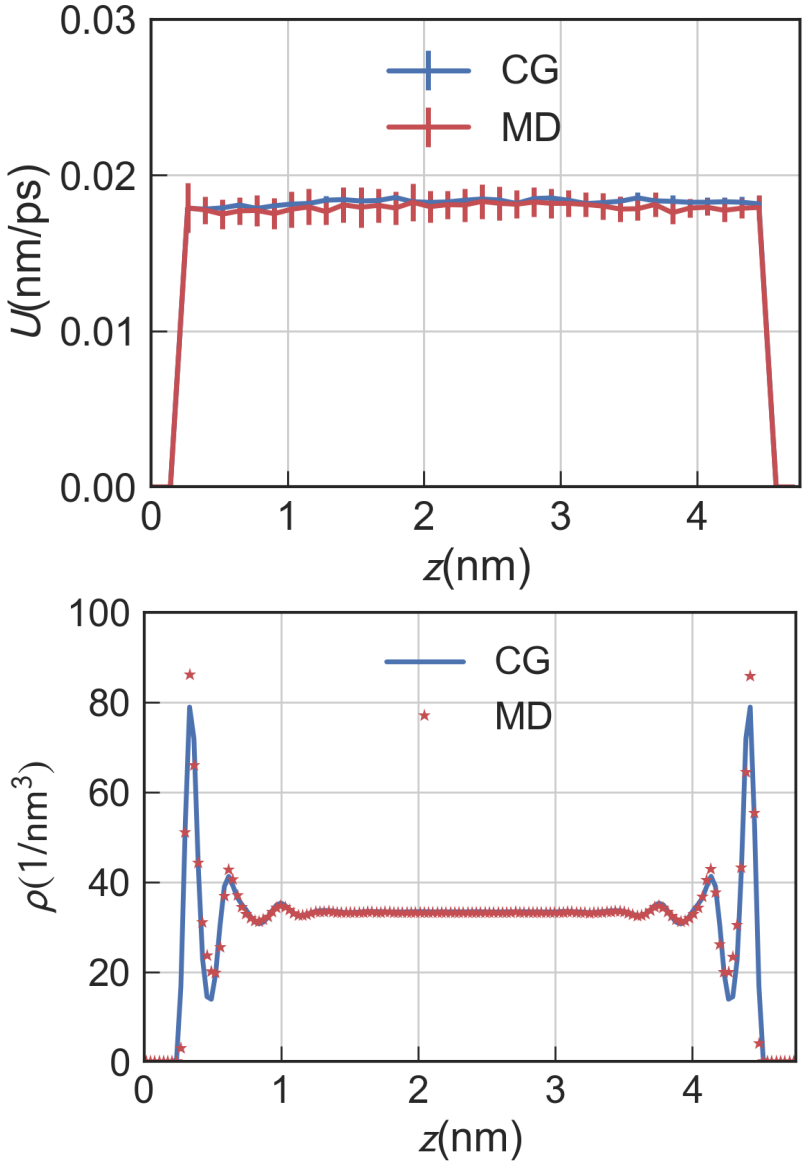

Figure 4.6: Comparison of velocity and density profile between the AAMD and CG systems. $h = 15\sigma$ and $F_{drive} = 0.1$ J/mol.nm

The simulated velocity profiles will be compared to the continuum prediction based on calculated equilibrium properties. The reason behind this comparison is to check in which operating conditions will the CG model agree with the linear regime pre-

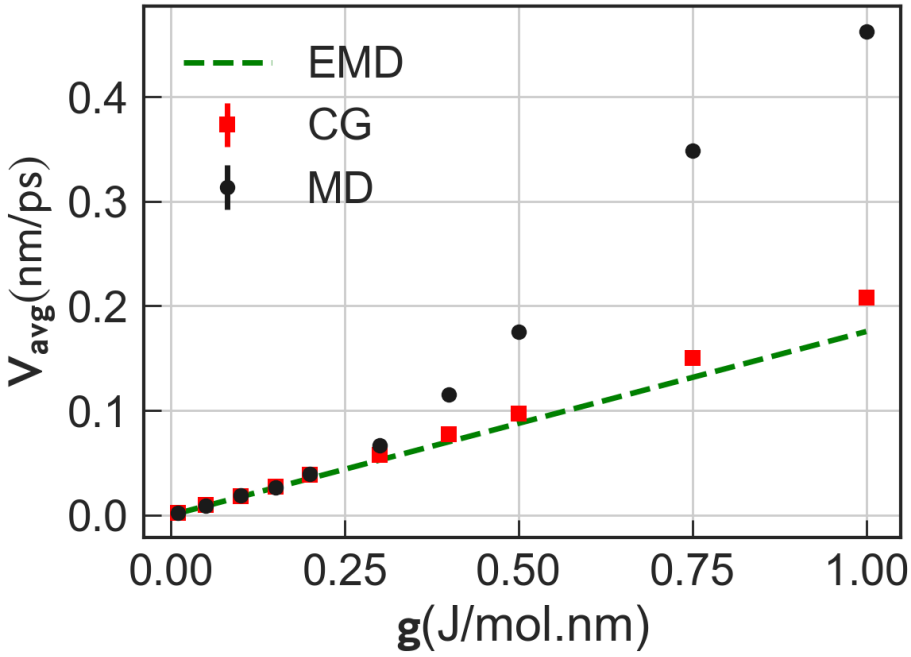

Figure 4.7: The average velocity V_{avg} in the 15σ channel as a function of gravity as predicted by the CGMD, AAMD, and EMD simulations.

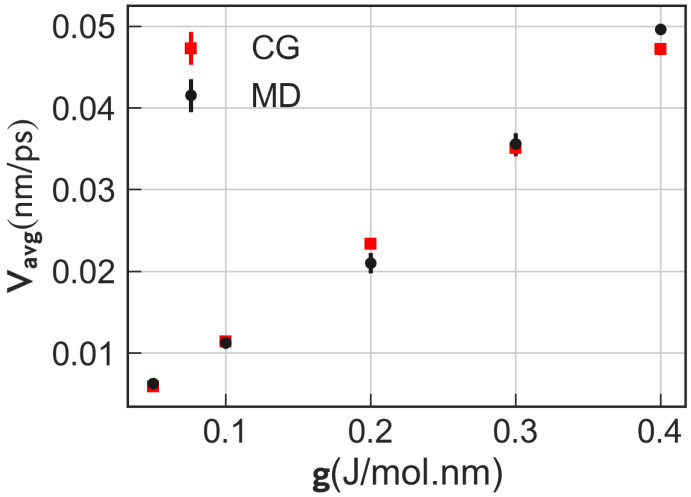

Figure 4.8: The average velocity V_{avg} in the 10σ channel as a function of gravity as predicted by the CGMD and AAMD simulations.

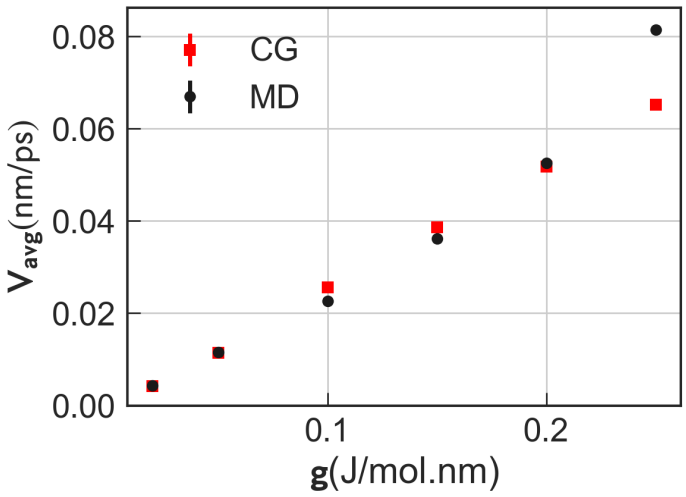

Figure 4.9: The average velocity V_{avg} in the 20σ channel as a function of gravity as predicted by the CGMD and AAMD simulations.

dicted using the same properties that CGMD matches. The continuum model is described in previous works extensively. Here a brief description will be made based on simplifying assumptions. First, since the flow velocity is plug-like in regimes simulated, the average velocity of the flow will be very close to the slip velocity as can be seen from figures 4.6, 4.10 and 4.11. Slip velocity in the linear regime with constant friction factor is computed as $V_{slip} = \frac{mg}{\zeta}$[31]. Based on the first assumption the average velocity is

$$V_{avg} = V_{slip} = \frac{mg}{\zeta} = \frac{F_{drive}}{\zeta}$$

. The previous equation will be referred to later as the equilibrium molecular dynamics (EMD) prediction. Figure 4.7 shows the good match between CGMD, AAMD and EMD predictions in the low-velocity regime. Hence the CG model has the same slip velocity that its equilibrium behavior was optimized to match.

The flow simulations in the different channels and conditions showed a good match between CGMD and AAMD simulations. In the 15σ channel, in which the model was developed, the agreement was exact in the low-velocity linear regime. Figure 4.7 shows the averaged velocity V_{avg} as a function of gravity applied in the 15σ channel.

The linear increase in average velocity stops at $g = 0.2$J/mol.nm for the AAMD system after which the velocity diverges from the EMD prediction. Figures 4.9 and 4.8 compares the prediction of CGMD and AAMD in the 10σ and 20σ channels. Again the same trend persists, where the transport predicted from the CG model is in good agreement with the AAMD system in the low-velocity regime, but then starts to deviate at higher velocities. For the three systems studied, the AAMD slip velocity starts to deviate from the equilibrium prediction at around 50m/s.

The CGMD simulations were approximately 15 times faster than the AAMD simulations. The mapping of the atomistic system into the coarse-grained system reduced the number of atoms and removed the electrostatic interaction between the atoms. As a result, the computational resources required for the same number of steps was about 4 times less for the CGMD system. The additional factor of 5 comes from the fact that the CGMD model can be run at a time step of 5fms compared to 1fms for the AAMD simulations. The benefit of this speedup is most significant for the flow simulations with low velocities. It is known that for the experimentally relevant velocity range of cm/s, the AAMD simulations have a poor signal to noise ratio. The reason is that the streaming velocity is close to the thermal velocity, and therefore the AAMD simulations will require longer simulation times to get well-converged results. Hence, with the 15 times speedup the great accuracy at low velocity, the CGMD model becomes more suitable for studying experimentally relevant flows.

In summary, the CG model was able to match the key transport properties and simulate accurate nano-scale transport faster in the low-velocity regime. The friction factor ζ and viscosity μ of the CGMD system were within 1% of the AAMD result, and the averaged relative error in density was less than 7%. The good match in the equilibrium properties led to a good match in the transport behavior. The CGMD reasonably predicted the velocity profile of the AAMD system, in the regime where the AAMD behavior was linear that extends over all the experimentally rel-

evant flow conditions. Finally, the CGMD model was about 15 times faster than AAMD simulations.

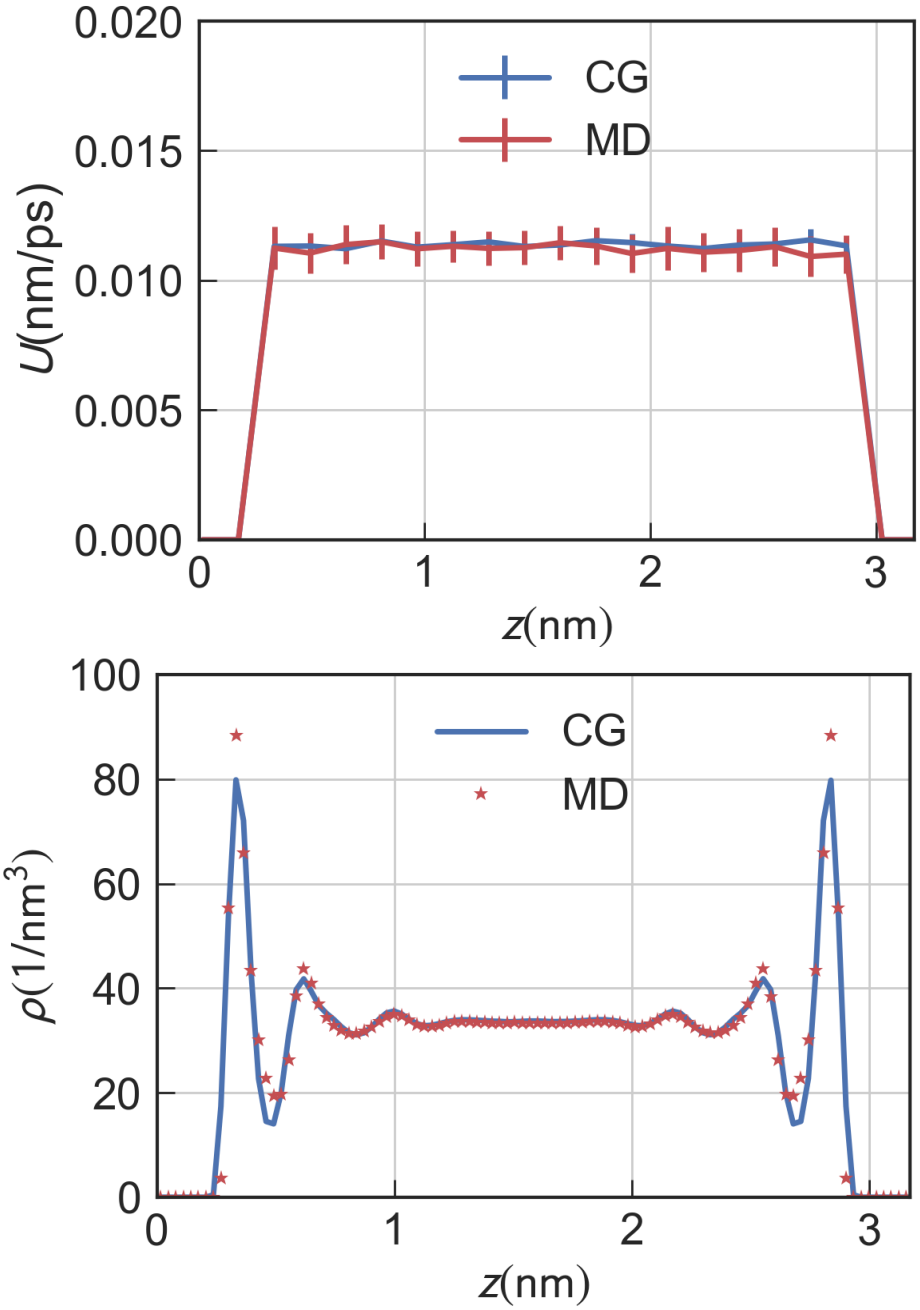

Figure 4.10: Comparison of velocity and density profile between the AAMD and CG systems. $h = 10\sigma$ and $g = 0.15$ J/mol.nm

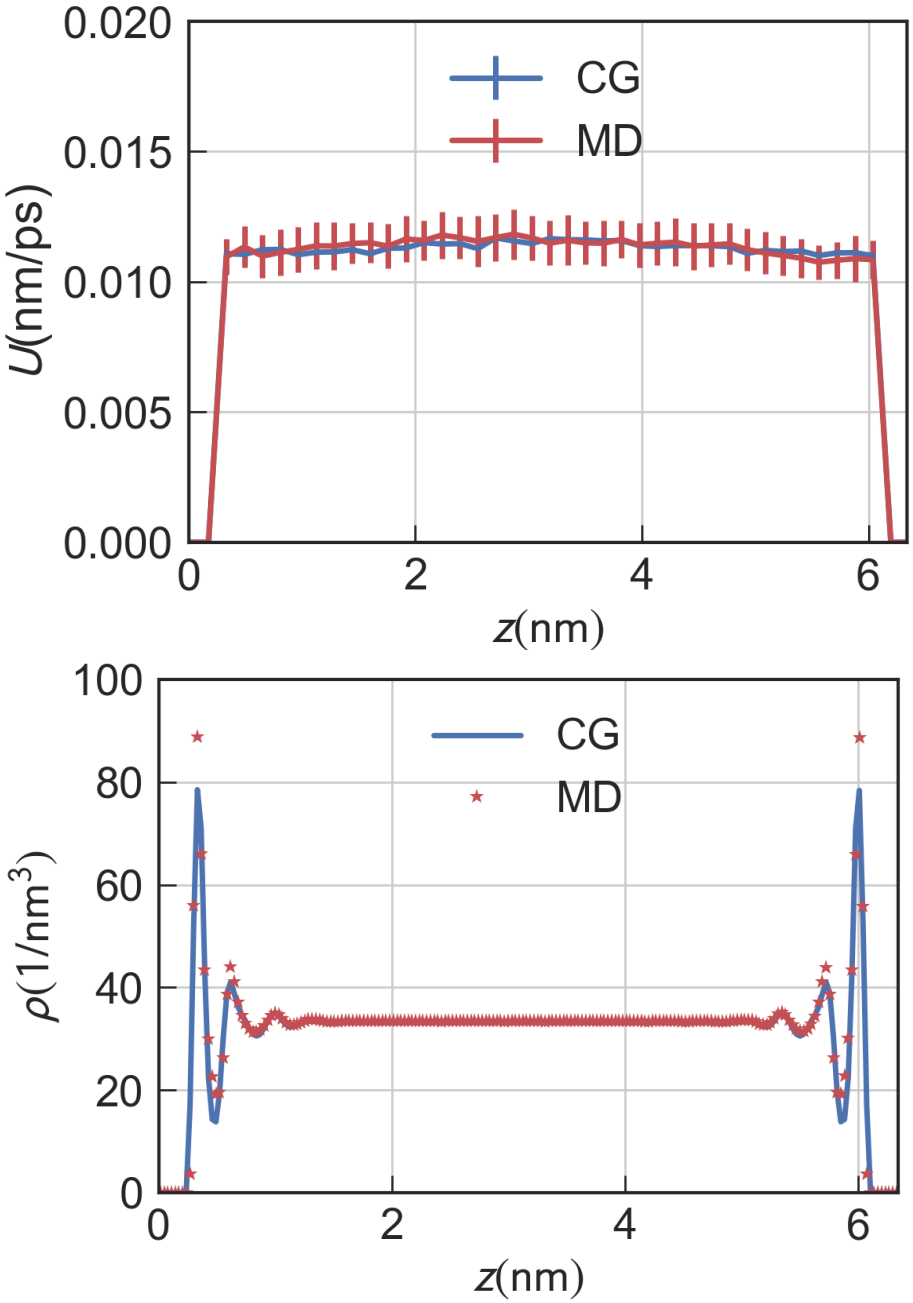

Figure 4.11: Comparison of velocity and density profile between the AAMD and CG systems. $h = 20\sigma$ and $g = 0.05$ J/mol.nm

CHAPTER 5

CONCLUSION AND FUTURE WORK

5.1 Conclusion

The main goal of this work was to develop a coarse-grained molecular dynamics model that is able to simulate transport in nano-fluidic systems. After developing the model and determining the required targets, an optimization scheme was formulated to find a parameter set of the model which achieve the set targets. The novelty of this CG model is that unlike other CG methods that replicate structure in nano-confinement, this model was designed to match friction factor and bulk viscosity as well. It was shown in this work that by matching structural and dynamical properties the CG model was able to simulate transport accurately in the linear regime compared to all-atom molecular dynamics.

The model was applied to water in the graphene nano-channel system. The results came such that the targets (density layering, friction factor, and bulk viscosity) were matched with the AAMD system by a multi-step optimization using the downhill simplex algorithm. In addition to matching density layering, the CG model matched friction factor simultaneously. Moreover, by carefully setting the thermostat properties, the bulk viscosity of CG water was matched with AAMD water. Using the developed model it was possible to simulate transport accurately and 15 times faster than AAMD in the low-velocity linear regime. Since in this experimentally relevant operation domain AAMD simulations are prohibitively slow, the developed model

will enable researchers to simulate these flows accurately and with a more reasonable computational cost.

5.2 Future Work

The accuracy of the model can be improved by changing the potential form and thermostat used. One of the main shortcomings of the model was to simulate transport at high shear rates where the molecular dynamics simulations start to deviate from linear regime behavior. The first challenge here will be to characterize the non-linear behavior efficiently, to be able to optimize the model to achieve it. The second challenge will be to change the model so that it will be able to match the low-velocity and high-velocity regime simultaneously. One possibility will be to replace the traditional DPD thermostat with a more versatile thermostat where the dissipative force will have an extra component. The effect of such thermostat should be studied to check how it can improve the accuracy of the current model. Another possibility will be to change the potential form to a numerical form such as a cubic spline. The suggested modifications may be necessary to include for other systems to achieve a similar performance that the current model achieved for the water-graphene system. The second front on which research should be done is the model efficiency. The reason behind doing coarse-graining is to simulate systems faster. Although this method was 15 times faster than MD, a higher speedup may be possible. Researchers that use DPD to simulate mesoscale flows, usually combine more than one fluid molecule to form one CG particle. A similar attempt can be made for this model. New wall-fluid and fluid-fluid potentials should be optimized again to match the target properties. Finally, the optimization algorithm should be studied more to decrease the computational cost associated with finding the optimal parameter set. Although the optimization is a one-time procedure for every system, a more efficient algorithm can find better solution points, which may be necessary for systems where a good initial parameter set is hard to find causing the simplex algorithm to get stuck at

non-satisfactory points. The challenge posed here is that the objective function is highly non-linear and requires a molecular dynamics simulation to evaluate it. Hence any optimization algorithm used will have to be gradient-free, where no gradient definition is necessary.

REFERENCES

[1] BJ Alder, DM Gass, and TE Wainwright. Studies in molecular dynamics. viii. the transport coefficients for a hard-sphere fluid. *The Journal of Chemical Physics*, 53(10):3813–3826, 1970.

[2] Juan R Perilla, Jodi A Hadden, Boon Chong Goh, Christopher G Mayne, and Klaus Schulten. All-atom molecular dynamics of virus capsids as drug targets. *The journal of physical chemistry letters*, 7(10):1836–1844, 2016.

[3] Isabella Daidone, Andrea Amadei, Danilo Roccatano, and Alfredo Di Nola. Molecular dynamics simulation of protein folding by essential dynamics sampling: folding landscape of horse heart cytochrome c. *Biophysical journal*, 85(5):2865–2871, 2003.

[4] Liliya Euro, Outi Haapanen, Tomasz Róg, Ilpo Vattulainen, Anu Suomalainen, and Vivek Sharma. Atomistic molecular dynamics simulations of mitochondrial dna polymerase γ: Novel mechanisms of function and pathogenesis. *Biochemistry*, 56(9):1227–1238, 2017.

[5] Mohammad Heiranian, Amir Barati Farimani, and Narayana R Aluru. Water desalination with a single-layer mos 2 nanopore. *Nature communications*, 6:8616, 2015.

[6] Zachary Grant Mills, Wenbin Mao, and Alexander Alexeev. Mesoscale modeling: solving complex flows in biology and biotechnology. *Trends in biotechnology*, 31(7):426–434, 2013.

[7] Y G Yingling and B J Garrison. Coarse-Grained Chemical Reaction Model. *Journal of Physical Chemistry B*, 108(6):1815–1821, 2004.

[8] Sergei Izvekov and Gregory A. Voth. Multiscale coarse graining of liquid-state systems. *Journal of Chemical Physics*, 123(13), 2005.

[9] Timothy C. Moore, Christopher R. Iacovella, and Clare McCabe. Derivation of coarse-grained potentials via multistate iterative Boltzmann inversion. *Journal of Chemical Physics*, 140(22), 2014.

[10] S. Y. Mashayak, Mara N. Jochum, Konstantin Koschke, N. R. Aluru, Victor Rühle, and Christoph Junghans. Relative entropy and optimization-driven coarse-graining methods in VOTCA. *PLoS ONE*, 10(7), 2015.

[11] Sergei Izvekov and Gregory A. Voth. Modeling real dynamics in the coarse-grained representation of condensed phase systems. *Journal of Chemical Physics*, 125(15), 2006.

[12] Chia-Chun Fu, Pandurang M. Kulkarni, M. Scott Shell, and L. Gary Leal. A test of systematic coarse-graining of molecular dynamics simulations: Transport properties. *The Journal of Chemical Physics*, 139(9):094107, 2013.

[13] P. J. Hoogerbrugge and J. M. V. A. Koelman. Simulating microscopic hydrodynamic phenomena with dissipative particle dynamics. *EPL (Europhysics Letters)*, 19(3):155, 1992.

[14] Daan Frenkel and Berend Smit. *Understanding molecular simulation: from algorithms to applications*, volume 1. Elsevier, 2001.

[15] Zhen Li, Xin Bian, Bruce Caswell, and George Em Karniadakis. Construction of dissipative particle dynamics models for complex fluids via the mori–zwanzig formulation. *Soft Matter*, 10(43):8659–8672, 2014.

[16] Aram Davtyan, James F. Dama, Gregory A. Voth, and Hans C. Andersen. Dynamic force matching: A method for constructing dynamical coarse-grained models with realistic time dependence. *Journal of Chemical Physics*, 142(15), 2015.

[17] Kerstin Falk, Felix Sedlmeier, Laurent Joly, Roland R. Netz, and Lydéric Bocquet. Molecular origin of fast water transport in carbon nanotube membranes: Superlubricity versus curvature dependent friction. *Nano Letters*, 10(10):4067–4073, 2010.

[18] Kai Huang and Izabela Szlufarska. Green-Kubo relation for friction at liquid-solid interfaces. *Physical Review E - Statistical, Nonlinear, and Soft Matter Physics*, 89(3):1–10, 2014.

[19] Eugene Helfand. Transport coefficients from dissipation in a canonical ensemble. *Phys. Rev.*, 119:1–9, Jul 1960.

[20] William G. Hoover. Canonical dynamics: Equilibrium phase-space distributions. *Phys. Rev. A*, 31:1695–1697, Mar 1985.

[21] John Edward Jones. On the determination of molecular fields.ii. from the equation of state of a gas. *Proc. R. Soc. Lond. A*, 106(738):463–477, 1924.

[22] Eric E Keaveny, Igor V Pivkin, Martin Maxey, and George Em Karniadakis. A comparative study between dissipative particle dynamics and molecular dynamics for simple-and complex-geometry flows. *The Journal of chemical physics*, 123(10):104107, 2005.

[23] Pep Espanol and Patrick Warren. Statistical mechanics of dissipative particle dynamics. *EPL (Europhysics Letters)*, 30(4):191, 1995.

[24] Ravi Bhadauria and N. R. Aluru. A quasi-continuum hydrodynamic model for slit shaped nanochannel flow. *The Journal of Chemical Physics*, 139(7):074109, 2013.

[25] John A Nelder and Roger Mead. A simplex method for function minimization. *The computer journal*, 7(4):308–313, 1965.

[26] Ira R Cooke, Kurt Kremer, and Markus Deserno. Tunable generic model for fluid bilayer membranes. *Physical Review E*, 72(1):011506, 2005.

[27] Sanjit K Das, Mukul M Sharma, and Robert S Schechter. Solvation force in confined molecular fluids using molecular dynamics simulation. *The Journal of Physical Chemistry*, 100(17):7122–7129, 1996.

[28] HJC Berendsen, JR Grigera, and TP Straatsma. The missing term in effective pair potentials. *Journal of Physical Chemistry*, 91(24):6269–6271, 1987.

[29] Paul P Ewald. Die berechnung optischer und elektrostatischer gitterpotentiale. *Annalen der physik*, 369(3):253–287, 1921.

[30] Victor Rhle, Christoph Junghans, Alexander Lukyanov, Kurt Kremer, and Denis Andrienko. Versatile object-oriented toolkit for coarse-graining applications. *Journal of Chemical Theory and Computation*, 5(12):3211–3223, 2009. PMID: 26602505.

[31] Sridhar Kumar Kannam, B. D. Todd, J. S. Hansen, and Peter J. Daivis. Slip flow in graphene nanochannels. *Journal of Chemical Physics*, 135(14), 2011.